Supporting Information

Self-passivated CuV_2O_6 as an universal photoelectrode material for reliable and accurate photoelectrochemical sensing

Boheng Dong,‡[ab] Tingting Sun,‡[c] Xiang Jiang,[b] Pengran Guo,[a] Guofen Yang[c] and Fuxian Wang[a]*

[a.] *Guangdong Provincial Key Laboratory of Emergency Test for Dangerous Chemicals, Institute of Analysis, Guangdong Academy of Sciences (China National Analytical Center, Guangzhou).*

[b.] *School of Chemistry and Chemical Engineering, South China University of Technology, Guangzhou 510640, China.*

c. Department of Gynecology, Sun Yat-Sen University First Affiliated Hospital, No. 58, Zhongshan Road II, 510080 Guangzhou, China.

*Corresponding Author, E-mail: wangfuxian@fenxi.com.cn.

Experimental Section

Materials and Reagents. Metallic copper (Cu, 99.995 %) and vanadium (V, 99.9 %) cylindrical sheet targets were purchased from ZhongNuo Advanced Material Technology Co., Ltd (China). 8-hydroxyquinoline (8-HQ) was obtained from Shanghai Aladdin Bio-Chem Technology Co., Ltd (China). Nafion (5 %) was supplied from DuPont (USA). L-arginine (L-Arg), L-valine (L-Val), L-glutamine (L-Glu), L-alanine (L-Ala), L-glycine (L-Gly), L-proline (L-Pro), ascorbic acid (AA) and glutaraldehyde (GLD) were purchased from Shanghai Macklin Biochemical Co., Ltd (China). Chitosan (CS) was obtained from Sinopharm Chemical Reagent Co., Ltd (China). CEA, monoclonal antibody to CEA (anti-CEA), AFP, monoclonal antibody to AFP (anti-AFP), and prostate specific antigen (PSA) were obtained from Shanghai Linc-Bio Science Co., Ltd (China). Bovine serum albumin (BSA) was brought from CUSABIO (Cusabio Biotech, Wuhan, China).

Preparation of CuV_2O_6 and CuO Photoelectrode. The CuV_2O_6 and CuO thin photoelectrodes were deposited on the fluorine-doped tin oxide (FTO) coated glass substrate by direct-current reactive magnetron sputtering method. During film deposition, FTO was heated to 200 ℃ and kept rotating at 20 r/min. The flow ratio of argon and oxygen was 23:7. The pressure in the vacuum chamber was maintained at 1.2 Pa and the deposition time was 2700 s. Specifically for CuO, Cu target was sputtered at a power of 15 W. For CuV_2O_6, the sputtering power of Cu target and V target were 15 W and 350 W, respectively. After deposition, the photoelectrodes were finally calcinated in air at 450 ℃ for 1 h.

Fabrication of the Sensor. The construction method of the L-arginine sensor was as follows. First, the 8-HQ was loaded on the CuV_2O_6 photoelectrode by spin coating. 20 μL of 8-HQ ethanol solution containing 0.5 % Nafion was dropped onto the photoelectrode and then the photoelectrode was rotated at a speed of 1000 r/min for 18s. Finally, CuV_2O_6/8-HQ was incubated with L-arginine solution at a certain concentration (10^{-5} ~ 10^{-3} M).

The fabrication of the CEA and AFP sensor was as follows. Firstly, 0.5 % CS in 1 % acetic acid solution was coated on the CuV_2O_6 photoelectrode using a spin coating method with a spinning speed of 2000 r/min and dried at room temperature. Subsequently, CuV_2O_6/CS was immersed in 5% GLD, kept at room temperature for 30 minutes, and then washed with deionized water. Next, the CuV_2O_6/CS/GLD was immersed in 50 μL of anti-CEA (50 μg/mL) or anti-AFP (50 μg/mL) for 12 h

at 4 ℃, and then immersed in 50 μL of 1 % BSA for 1 h at 4 ℃ to block the nonspecific active binding sites. Finally, CuV_2O_6/CS/GLD/antibody was incubated with CEA or AFP solution at a certain concentration (10^{-3} ~ 10^3 ng/mL) for 1h at 4 ℃.

Material Characterization. The scanning electron microscope (SEM) measurements were carried using a HITACHI SU8220 scanning electron microscope at an acceleration voltage of 5 kV. The X-ray diffraction (XRD) was carried out to investigate the crystal structures of the CuV_2O_6 film using a Rigaku SmartLab X-ray diffraction with Cu Kα radiation (λ = 0.154 nm). UV−vis diffuse reflectance spectra was recorded by a HITACHI U-4100 spectrophotometer. Attenuated total internal reflectance Fourier transform infrared (ATR-FTIR) tests were carried out on the Thermo NICOLET 150 FT-IR. X-ray photoelectron spectroscopy (XPS) with Al Kα X-rays (hν = 1486.6 eV) radiation (Thermo Scientific K-Alpha Nexsa) was used to analyse the chemical states on the surface.

Photoelectrochemical Measurements. The PEC measurements were carried using an CHI70E electrochemical workstation (Shanghai Chenhua Instrument Co., Ltd., China) in a three-electrode configuration with the PEC sensor as working electrode, an Ag/AgCl reference electrode and a platinum sheet counter electrode. A xenon lamp (CEL-HXF300, CEAULIGHT, China) with a AM1.5 filter was used as an illumination source. By using neutron filters with different optical densities and bandpass filters, PEC tests were carried out at the 0.1 AM1.5 (10 mW/cm^2). The detection of L-arginine was carried out at a potential of 0.4 V vs. Ag/AgCl, and borate buffer solution (BBS, pH=9.0) containing 0.1 M H_3BO_3 and 0.05 M NaOH was used as the electrolyte. The detection of CEA and AFP was carried out at a potential of 1.2 V vs. Ag/AgCl, and 0.1 M phosphate buffer solution (PBS, pH=7.4) was used as the electrolyte. Specifically for p-type CuO that shows negative photo-response, the absolute value of the photocurrent density was used in the results and discussions.

Real Sample Collection and Determination. Grapes and apples were purchased from the supermarket, and then squeezed by a juicer to obtain fruit samples. The human serum samples were obtained from the local hospital, and the research has been approved by the Ethics Committee of the First Affiliated Hospital of Sun Yet-sen University (ethics approval no. 308-2016-03-01). The juice was centrifuged at 6000 r/min for 10 min, and then the supernatant was taken. The real samples were diluted with electrolyte to an appropriate concentration and then tested. HPLC (Agilent 1260) was

used to test the concentration of L-arginine in juice and human serum as a reference. Chemiluminescence (CL) method was used to detect the content of CEA and AFP in human serum as a reference.

Optimization of CuV_2O_6 preparation parameters

By changing the power of the V target while fixing the power of Cu target at 15 W, the samples with different ratios of Cu and V can be obtained. The PEC performance of the sample was the best when the power of the Cu target was 15 W and the power of the V target was 350 W, as shown in Figure S1a. Furthermore, we have also optimized the film thickness. By changing the deposition time, the samples with different thicknesses can be obtained. As shown in Figure S1b, the highest PEC performance was achieved when the deposition time was 2700 s.

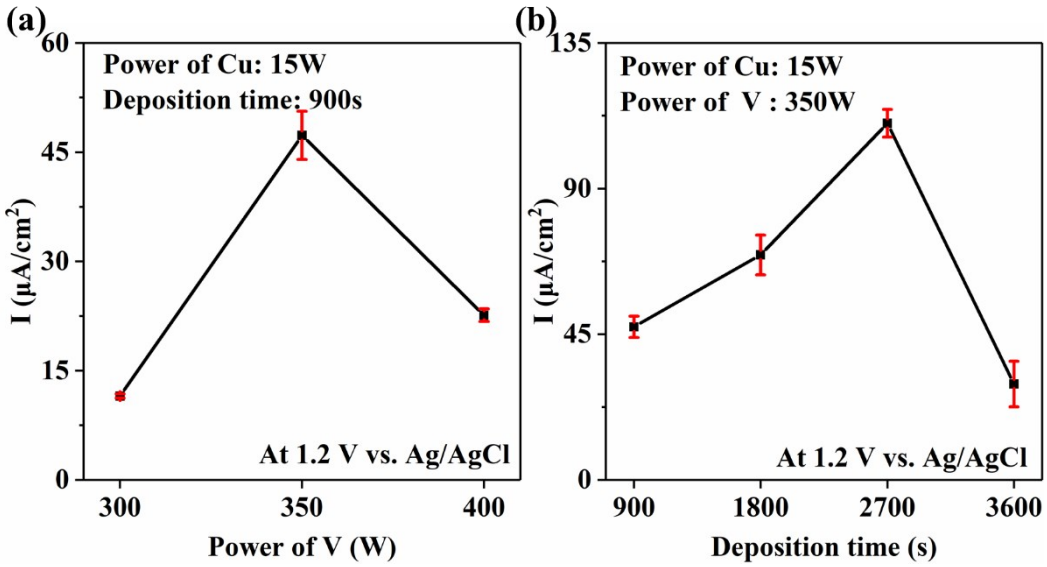

Figure S1. (a) Photocurrent density of samples prepared under different V power; The power of Cu is 15 W, and the deposition time is 600 s. (b) Photocurrent density of CuV_2O_6 photoelectrode with different deposition time; The power of Cu and V are 15 W and 350 W, respectively.

Semiconductor properties of CuV_2O_6

Figure S2 shows the photocurrent under different biased penitential.

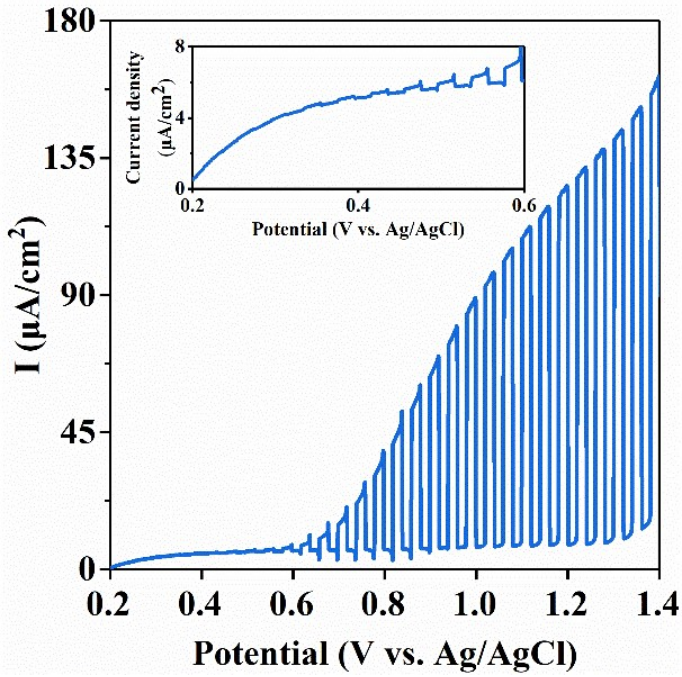

Figure S2. The chopped LSV scans for CuV_2O_6 photoelectrodes. The measurements were performed in PBS.

Mott-Schottky tests were performed in PBS and BBS. The flat band potential of CuV_2O_6 was estimated to be at 0.77 V vs. RHE, as shown in Figure S3. The positive slope of Mott−Schottky plots and the positive photocurrent indicated that CuV_2O_6 shows n-type semiconductor behavior.

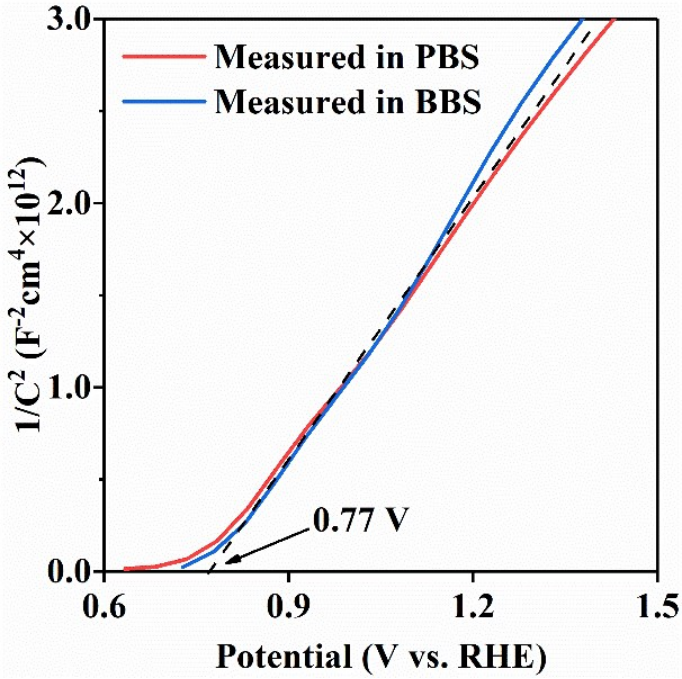

Figure S3. Mott–Schottky plots for CuV_2O_6. The measurements were performed in PBS and BBS.

The theoretical calculation suggested that the Fermi level of CuV_2O_6 is less than 0.08 eV (~3KT) away from the conduction band edge. Based on the Mott-Schottky results and the bandgap value obtained from the Tauc plot (inserted photograph of Figure 1c), the band diagram of CuV_2O_6 was sketched, as shown in Figure S4

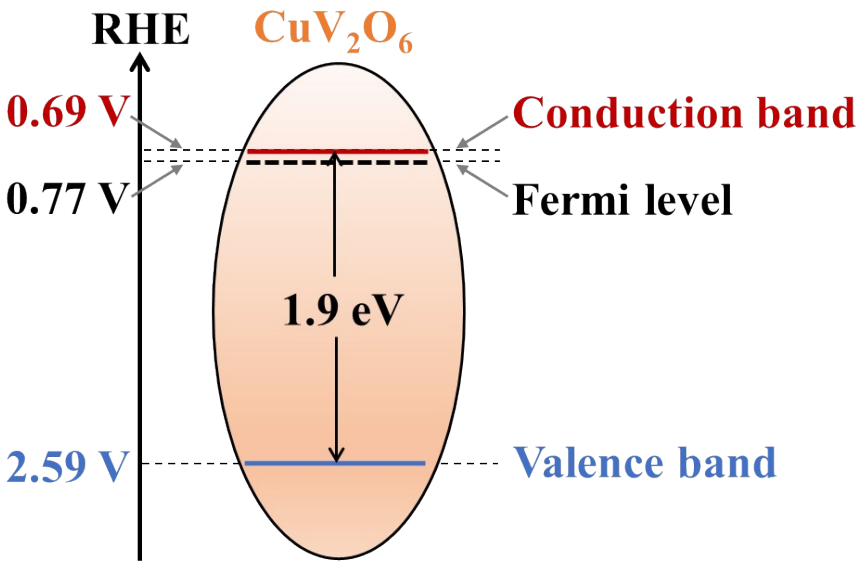

Figure S4. Estimated band diagrams of CuV_2O_6.

Attenuated total internal reflectance Fourier transform infrared (ATR-FTIR) was used to analyse the surface composition of the photoelectrode, as shown in Figure S5. Compared with CuV_2O_6, the CuV_2O_6/8-HQ showed new absorption peaks that matched well with the standard spectrum of 8-HQ[1], demonstrating the successful loading of 8-HQ on top of CuV_2O_6. After incubating the CuV_2O_6/8-HQ in L-arginine, a new absorption peak appeared at 1680 cm^{-1}, which can be attributed to the out-of-plane bending of NH_2 group in L-arginine[2], suggesting that L-arginine has been successfully anchored onto the surface of CuV_2O_6/8-HQ.

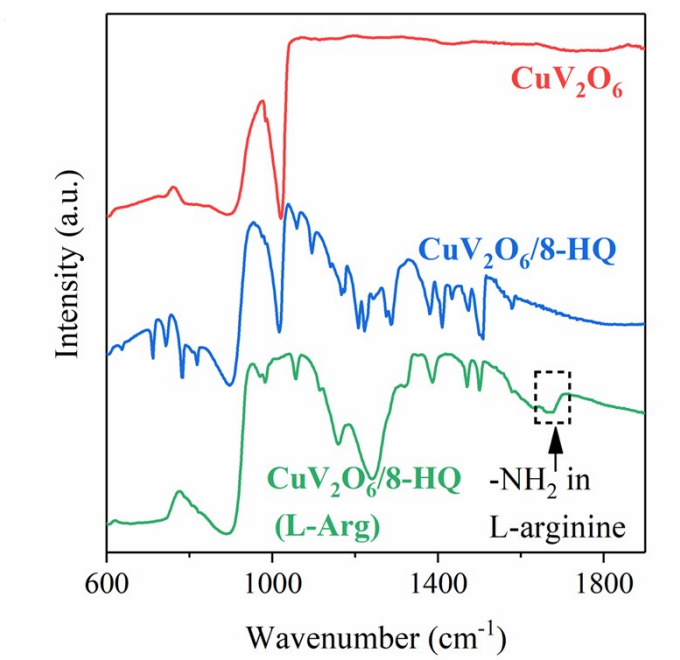

Figure S5. IR spectra for CuV_2O_6, CuV_2O_6/8-HQ and CuV_2O_6/8-HQ (L-arginine). CuV_2O_6/8-HQ (L-arginine) represents the CuV_2O_6/8-HQ after incubation in L-arginine.

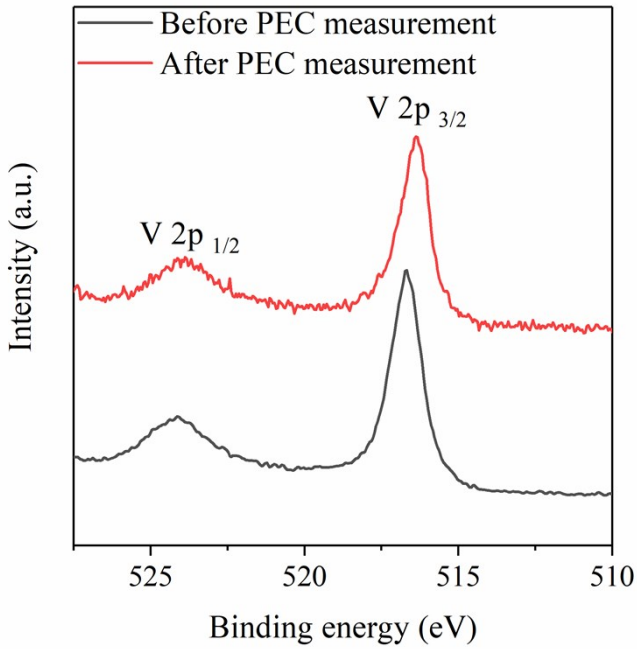

Figure S6. High-resolution XPS of the V 2p for CuV_2O_6 photoelectrode before and after PEC measurement.

Optimal Conditions for the CuV_2O_6/8HQ Sensor.

In order to achieve better PEC signal of the L-arginine sensor, the potential of the PEC measurement (Figure S7a), the power density of the illumination (Figure S7b), the load of 8-HQ (Figure S7c) and the incubation time of CuV_2O_6/8-HQ in L-arginine (Figure S7d) were optimized. I_0 and I are the values of photocurrent density before and after incubation in L-arginine respectively, and I/I_0 was used to assess the sensitivity of the PEC signal. As shown in Figure S7a, I/I_0 reached a maximum value of 10.7 at 0.4 V vs. Ag/AgCl, which was selected as the measurement potential. When the PEC measurements were performed with a power density of 10 mW/cm^2, I/I_0 achieved the maximum value, as shown in Figure S7b. It is crucial to load suitable amount of 8-HQ on CuV_2O_6. 20 μL 8-HQ precursor solution with different concentrations was spin-coated on CuV_2O_6 to control the total load of 8-HQ. As shown in Figure S7c, the PEC signal increased significantly as the concentration of 8-HQ precursor increased from 10mM to 100mM, and levelled at approximately 6.5 $\mu A/cm^2$ as the concentration of 8-HQ precursor further increased from 100 to 300 mM. Therefore, we chose to coat 20 μL of 200 mM 8-HQ on CuV_2O_6. Incubation time is also an important parameter. Under the premise that the reaction between 8-HQ and L-arginine is saturated, the incubation time should be reduced as much as possible to improve the detection efficiency. As shown in Figure S7d, the PEC signal increased significantly after CuV_2O_6/8-HQ was incubated in 100 μM L-arginine solution for 1 min. After 10 min incubation, the PEC signal reached a plateau, indicating that the reaction was saturated, so 10 min was chosen as the incubation time. For comparison, the PEC sensor reported in the literatures[3, 4] usually take 30~90 min to reach the reaction saturation, demonstrating the advantage of our L-arginine sensor for fast detection.

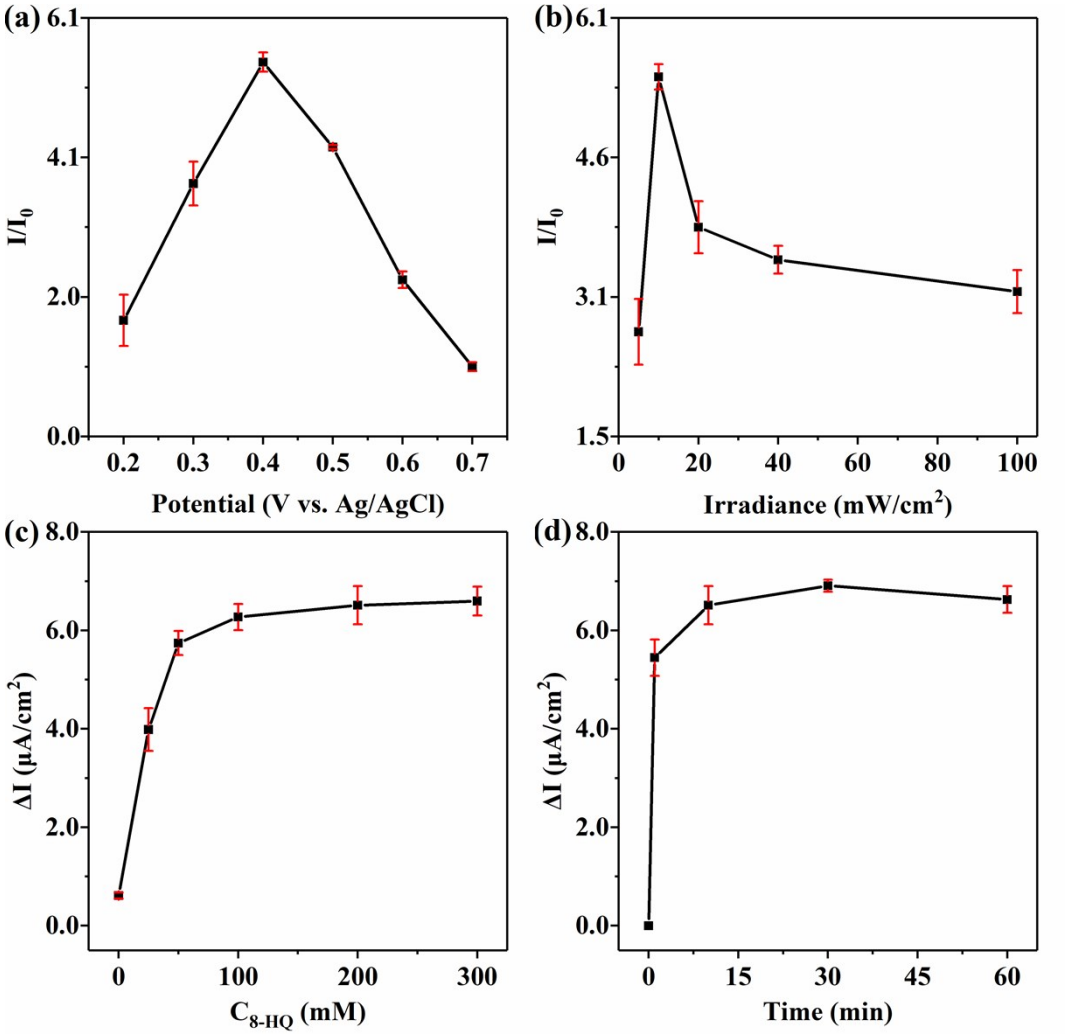

Figure S7. PEC measurement under (a) different potential and (b) various power density of the illumination; Photocurrent outputs of (c) CuV_2O_6 photoelectrode modified with different concentrations of 8-HQ, and (d) CuV_2O_6/8-HQ with varied incubation time. I_0 and I denote the values of photocurrent density before and after incubation in L-arginine, respectively; $\Delta I = I - I_0$.

Electrolyte for CuV_2O_6-based sensor

As shown in Figure S8a and S8b, it takes 10 min and 60 min for the CuV_2O_6/8-HQ sensor to reach saturated incubation of L-arginine in BBS and PBS solution, respectively. In order to accelerate the detection efficiency, BBS was chosen as the electrolyte for L-arginine detection. Neutral electrolyte (PBS) was used for the detection of CEA and AFP because antibodies and antigens can be easily inactivated under alkaline conditions[5].

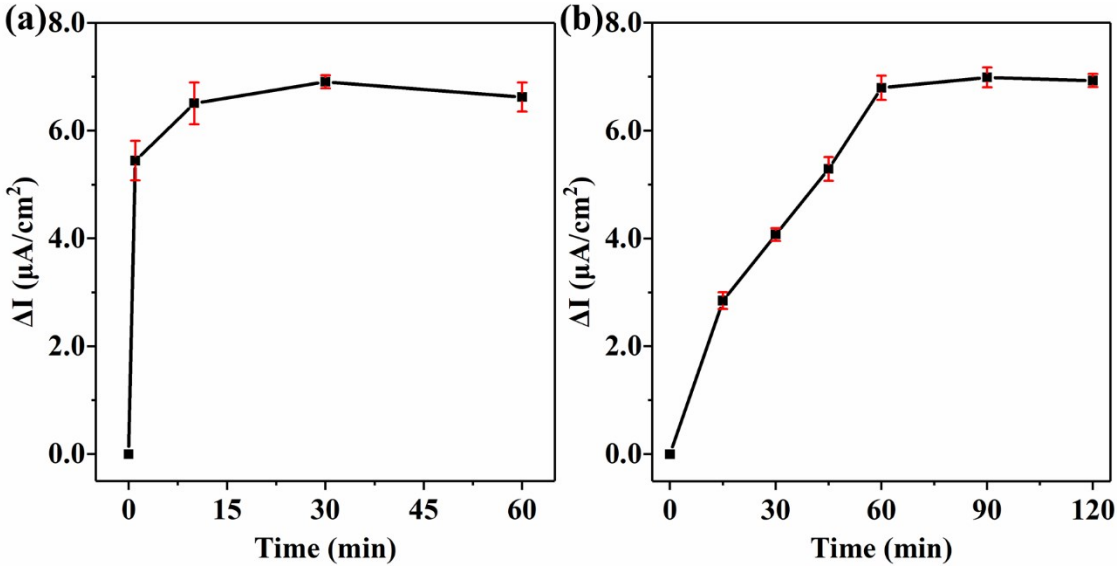

Figure S8. CuV_2O_6/8-HQ was incubated in (a) BBS and (b) PBS containing 100 μM L-arginine with varied incubation time.

Photoelectron oxidation of L-arginine

According to previous researches, L-arginine can be possibly oxidized as follows[6, 7]:

$$RCH(NH_2)COOH + 2h^+ \rightarrow RCH = NH + CO_2 + 2H^+ \quad (1)$$

$$RCH = NH + 2h^+ \rightarrow RC \equiv N + 2H^+ \quad (2)$$

$$\{RCH = NH + H_2O \rightarrow RCH = O + NH_3\} \quad (3)$$

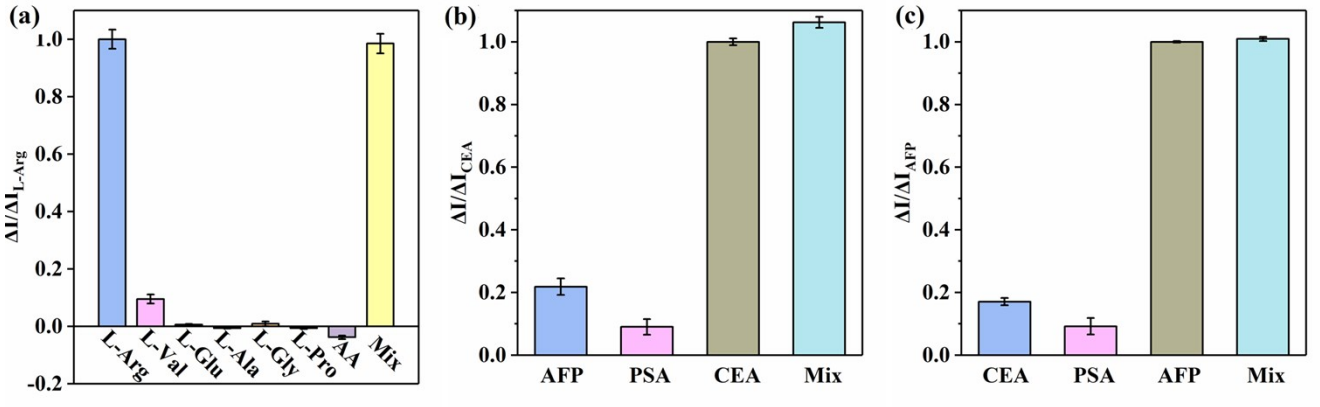

Figure S9. (a) PEC response of the L-arginine sensor to 100 μM of L-Arg, L-Val, L-Glu, L-Ala, L-Gly, L-Pro, AA and mixture; (b) PEC response of the CEA sensor to 1 ng/mL of CEA and 10 ng/mL AFP, PSA and mixture; (c) PEC response of the AFP sensor to 1 ng/mL of AFP and 10 ng/mL CEA,

PSA and mixture. The biased potential of the PEC measurement is 0.4 V, 1.2 V and 1.2 V (vs. Ag/AgCl) for L-arginine, CEA and AFP sensor, respectively.

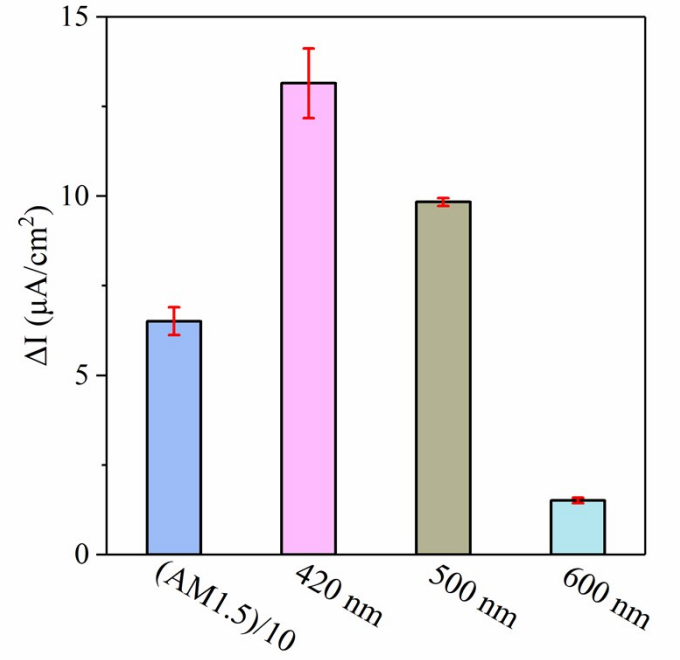

Figure S10. The PEC response of CuV_2O_6/8-HQ sensor under different light source with a power density of 10 mW/cm^2. The biased potential of the PEC measurement is 0.4 V (vs. Ag/AgCl).

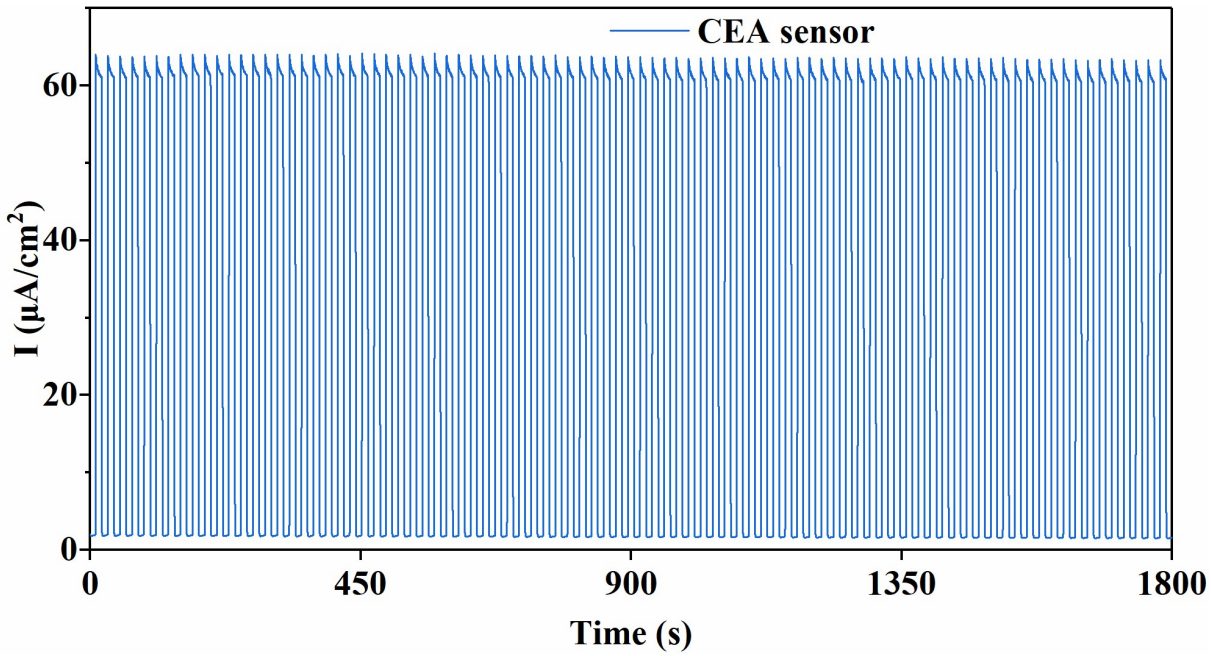

Figure S11. The stability of CuV_2O_6-based CEA sensor in PBS electrolyte at 1.2 V vs. Ag/AgCl.

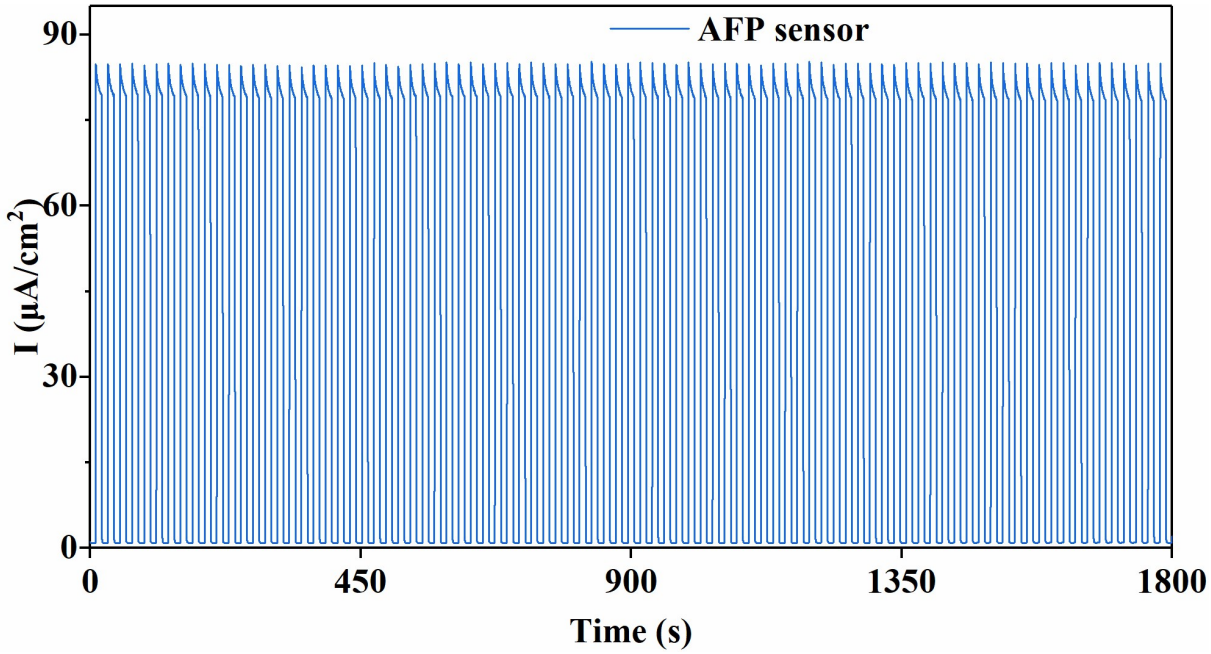

Figure S12. The stability of CuV_2O_6-based AFP sensor in PBS electrolyte at 1.2 V vs. Ag/AgCl.

Table S1. Photo-corrosion of the copper-oxide based PEC sensor in the literatures[3, 4, 8-13]

Material	Test duration (min)	Normalized photo-corrosion rate (%/min)	References
CuO-Cu_2O	15	0.70	3
CuO	6	1.00	4
$CuBi_2O_4$/Au	5	0.85	8
$CuBi_2O_4$	5	1.02	9
Ti_3C_2/Cu_2O	6.5	1.69	10
CuO-g-C_3N_4	10	0.74	11
CuO	6.5	0.80	12
Cu_2O-CuO	2	1.73	13
CuO	30	1.08	This work
CuV_2O_6	30	0.02	This work

Note: normalized photo-corrosion rate = $(I_{start} - I_{end}) / (I_{start} \times \text{Test duration})$.

Table S2. Comparison of different methods for L-arginine determination[14-21]

Type of transducers	Bio-components	Working electrode	Noble metal free	Linear range (M)	Detection limit	Reference
Potentiometric	Arginase/urease	Glossy carbon electrode	Yes	$10^{-5} \sim 10^{-3}$	-	14
Amperometric	L/D- arginine oxidase	Graphite teflon electrode	Yes	$10^{-4} \sim 10^{-3}$	3.3×10^{-5}	15
Conductometric	Arginase/urease	Au coated ceramic plate	No	$10^{-4} \sim 1.4\times10^{-3}$	2.5×10^{-5}	16
Amperometric	Arginase/urease	PANi composite Pt electrode	No	$10^{-6} \sim 10^{-4}$	3.8×10^{-5}	17
Optical	Crude arginine deiminase	-	-	$10^{-4} \sim 1$	1.0×10^{-5}	18
Amperometric	Arginine deiminase	PANi composite Pt electrode	No	$3\times10^{-6} \sim 2\times10^{-4}$	1.0×10^{-6}	19
Cyclic voltammetry	8-HQ	Au electrode	No	$2\times10^{-5} \sim 10^{-4}$	-	20
Conductometric	Arginase/urease	Au interdigital electrode	No	$10^{-5} \sim 4\times10^{-3}$	5.0×10^{-7}	21
PEC	8-HQ	CuV_2O_6	Yes	$1\times10^{-5} \sim 1\times10^{-3}$	4.0×10^{-6}	This work

Table S3. Determination of L- arginine in fresh grape juice, apple juice and human serum by CuV_2O_6/8-HQ sensor

Sample	HPLC (μM)	Spiked (μM)	PEC (μM)	Recovery rate (%)	RSD (%)
Grape juice	35.98	0	36.81	-	2.25
	35.98	100	133.39	97.41	-7.20
Apple juice	29.18	0	31.19	-	6.89
	29.18	100	127.86	98.68	-4.52
Human serum	40.23	0	40.79	-	1.39
	40.23	100	137.53	97.30	-6.71

RSD = (PEC - Spiked - HPLC) / (HPLC) ×100 %, Recovery rate = (PEC - HPLC) / Spiked × 100 %.

Table S4. Determination of CEA and AFP in human serum by CuV_2O_6-based PEC sensors

PEC sensor		Detecting target	CL (ng/mL)	Spiked (ng/mL)	PEC (ng/mL)	Recovery rate (%)	RSD (%)
Photoelectrode material	Probe						
CuV_2O_6	anti-CEA	CEA	0.23	0.00	0.241	-	4.78
			0.23	1.00	1.218	99.8	-5.22
CuV_2O_6	anti-AFP	AFP	0.66	0.00	0.620	-	-6.06
			0.66	1.00	1.682	102.2	3.33

RSD = (PEC - Spiked - CL) / (CL) ×100 %, Recovery rate = (PEC - CL) / Spiked × 100 %.

References

1 G. Bozoklu, C. Marchal, J. Pécaut, D. Imbert and M. Mazzanti, *Dalton. Trans.*, 2010, **39**, 9112-9122.

2 S. Kumar and S. Rai, *Indian J. Pure Appl. Phys.*, 2010, **48**, 251-255.

3 S. Gu, X.-M. Shi, D. Zhang, G.-C. Fan and X. Luo, *Anal. Chem.*, 2021, **93**, 2706-2712.

4 Y. Zhu, Z. Xu, K. Yan, H. Zhao and J. Zhang, *ACS Appl. Mater. Interfaces*, 2017, **9**, 40452-40460.

5 G. Thiagarajan, A. Semple, J. K. James, J. K. Cheung and M. Shameem, *mAbs*, 2016, **8**, 1088-1097.

6 N. A. Hampson, J. B. Lee and K. I. Macdonald, *J. Electroanal. Chem. Interfacial Electrochem.*, 1972, **34**, 91-99.

7 M. Fleischmann, K. Korinek and D. Pletcher, *J. Electroanal. Chem. Interfacial Electrochem.*, 1971, **31**, 39-49.

8 L. Zhang, Y.-C. Zhu, Y.-Y. Liang, W.-W. Zhao, J.-J. Xu and H.-Y. Chen, *Anal. Chem.*, 2018, **90**, 5439-5444.

9 S. Lv, K. Zhang, Z. Lin and D. Tang, *Biosens. Bioelectron.*, 2017, **96**, 317-323.

10 M. Li, H. Wang, X. Wang, Q. Lu, H. Li, Y. Zhang and S. Yao, *Biosens. Bioelectron.*, 2019, **142**, 111535.

11 L. Mao, X. Xue, X. Xu, W. Wen, M.-M. Chen, X. Zhang and S. Wang, *Sens. Actuators B*, 2021, **329**, 129146.

12 Y.-L. Liu, Y.-C. Zhu, L.-B. Qu, R. Yang, X.-D. Yu and W.-W. Zhao, *ACS Appl. Bio Mater.*, 2019, **2**, 2703-2707.

13 Y. Fu, K. Zou, M. Liu, X. Zhang, C. Du and J. Chen, *Anal. Chem.*, 2019, **92**, 1189-1196.

14 N. Stasyuk, O. Smutok, G. Gayda, B. Vus, Y. Koval'chuk and M. Gonchar, *Biosens. Bioelectron.*, 2012, **37**, 46-52.

15 K. Kumar, T. Phathak and S. Walia, *J. Nat. Prod. Plant Resour.*, 2012, **2**, 494-499.

16 R. Domınguez, B. Serra, A. Reviejo and J. Pingarron, *Anal. Biochem.*, 2001, **298**, 275-282.

17 N. Verma, A. K. Singh and P. Kaur, *J. Anal. Chem.*, 2015, **70**, 1111-1115.

18 N. Verma, A. K. Singh and N. Saini, *Sens. Biosens. Res.*, 2017, **15**, 41-45.

19 M. T. Zhybak, L. Y. Fayura, Y. R. Boretsky, M. V. Gonchar, A. A. Sibirny, E. Dempsey, A. P. Turner and Y. I. Korpan, *Microchim. Acta*, 2017, **184**, 2679-2686.

20 M. He, J. Guo, J. Yang, Y. Yang, S. Zhao, Q. Xu, T. Wei, D. M. Ferraris, T. Gao and Z. Guo, *Electrochem. Commun.*, 2020, **118**, 106808.

21 O. Saiapina, S. Dzyadevych, N. Jaffrezic-Renault and O. Soldatkin, *Talanta*, 2012, **92**, 58-64.